

*Title:*

## **Direct Experimental Determination of Spatial Temperature Density and Mix for LTE Implosions**

*Author(s):*

**Greg Pollak**

*Submitted to:*

<http://lib-www.lanl.gov/la-pubs/00796537.pdf>

# Direct Experimental Determination of Spatial Temperature Density and Mix for LTE Implosions

Greg Pollak

*Los Alamos National Laboratory  
Los Alamos, New Mexico USA, 87545*

Advances in diagnostics development and related image analysis procedures are enabling a more fundamental understanding of Local Thermodynamic Equilibrium (LTE) implosions than previously possible. The most conceptually direct diagnostics suite utilizes a gated monochromatic imager (GMXI); streaked spectrometer, and an absolutely calibrated, time-integrated spectrograph. Although spectrometers are used, the imaged capsules should be in LTE, normally viewing continuum emission. The GMXI should be run in 2-color mode (for temperature ( $T$ ) and density ( $\rho$ ) only), or 3-color mode (including mix). Data analysis involves two other inputs; an opacity at the two or more colors; and the degree of absorption of the emitting region by relatively cold ablated material. The latter can be approximately obtained either from simulations, or from monochromatic detection of backlit imaging. The key concept is that the number of unknowns should equal the number of quantities measured. The unknowns are extracted by linearizing the line-of-sight (LOS) equation and iterating a multi-variable Newton procedure to convergence. We will present a detailed uncertainty analysis of diagnostic-related quantities by generating synthetic images from radiation-hydrodynamic (radhydro) simulations, passing these images through the data-analysis algorithm, and comparing output unknowns with the simulation results.

## 1) Introduction

This paper discusses how images recorded at different (x-ray) frequencies, combined with spatially-integrated spectroscopic information, can be manipulated to extract the space-dependent matter temperature ( $T$ ), mass density ( $\rho$ ), and mix fraction ( $f$ ). The technique is not restricted to spherical geometry, but that is both the most demanding case and the most relevant for ICF<sup>1,2</sup>. True 1-dimensional (D) spherical geometry is not required, but an axis of symmetry is (without utilizing tomographic reconstruction techniques). The technique is also not limited to LTE problems, but non-LTE high-density environments are difficult to obtain opacities for, because of optical depth, time-dependence and, most importantly, model complexity issues<sup>3</sup>. Also cryogenic capsule designs are usually approximately LTE. The frequency ranges used will be well above any bound-bound (BB) line energies for capsule materials, thus only continuum radiation (bound-free (BF) and free-free (FF)) will be viewed. The key issue determining the choice of diagnostics is that the number of measured variables should equal the number of unknowns. Since at least two fields ( $T$  and  $\rho$ ) and usually three ( $f$ ) are desired, the number of separate frequencies is 2 or 3 respectively. Although it is possible to preprocess multiple broad-band filtered images to obtain quasi-monochromatic images, a more straightforward approach would use a gated monochromatic imager<sup>4,5,6,7,8</sup>. In order to absolutely calibrate these MCP-based instruments, and to correct for inter-strip amplification variation, two other diagnostics are fielded simultaneously: a (time-integrated) spectrograph; and a streaked spectrometer.

A Newton algorithm is used to invert the set of non-linear LOS emission-absorption equations for these two or three images.

## 2) Uncertainty Analysis Results

As explained in the abstract, an uncertainty analysis has been performed using a radhydro code, (Lasnex), a postprocessor (TDG), and the algorithm described above (Newton). The inputs to the algorithm are: a spatial resolution (optimistically,  $5\mu\text{m}$ ); a fluence convergence criteria (15%), a gating time (80 ps); attenuation factors for each LOS and frequency due to cold, absorbing pusher material (from TDG); and initial guesses for the three fields at the radial points. In real life, these initial guesses would probably come from some temporal averaging of the results from a radhydro simulation. For this uncertainty analysis, this is the first step in the process, the second step being a few iterations of the Newton procedure with artificially tight fluence convergence criteria. The particular time slice displayed here started right at peak compression.

An important consideration in the algorithm is the location of the radial grid. As in any Abel inversion scheme, the detector resolution elements (pixels) are fixed in space and induce a set of radial resolution elements (also fixed in space), whose circular boundaries are tangential to the various LOS emanating from detector pixels. Thus the radial resolution thickness is determined by, and identical to, the detector resolution, and there is a one-to-one correspondence between pixels and radial units (zones). Another important consideration is that the algorithm works best sequentially, rather than holistically, i.e., the properties of the outermost zone are solved for first (using only the outermost LOS), then the next zone in is solved for using the corresponding LOS and the results of the first zone, etc.. These considerations make it clear that apriori knowledge (or assumptions) concerning mix can reduce the number of pixels for which the third color's fluence need be used—if a zone is assumed unmixed, then the corresponding pixel need only have information for 2 of the colors. The particular run analyzed here did not have any explicit mix, but fluence data at 3 colors is still needed for at least one pixel. This is because of the finite gating time, and the movement of the interface during that time. Any zones which contain the interface in this time interval will necessarily have a value of  $f$  different from 0 or 1, and thus the corresponding pixel will need all 3 colors. In the run used here, only one zone was “mixed”, and its corresponding pixel was located at  $\sim 25\mu\text{m}$ .

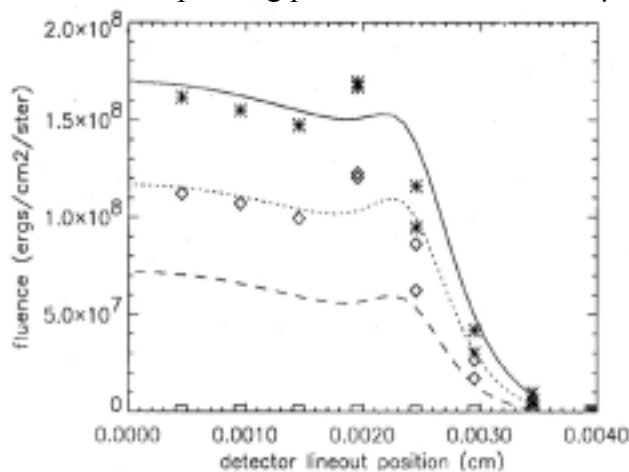


Fig. 1 Comparison of TDG fluence  
With Newton fluence

Figure 1 shows (postprocessor) lineouts of fluence for this capsule implosion at three different frequencies: 3keV; 3.5keV; and 4keV. Placed near the 3 curves are symbols which represent the values of fluence as calculated by Newton, both after the first iteration (i.e., using initial guesses); and after convergence. The convergence criteria was set at +15%. The asterisks correspond to 3keV; the diamonds to 3.5keV; and the squares to 4keV. In all cases the symbols nearest the corresponding curves are the converged values.

Figure 2 plots the ratio of radhydro densities at various times to the density at the start of gating integration. Placed nearby these curves are the initial-guess ratios (asterisks), and the converged ratios (diamonds). Figures 3 and 4 give corresponding results for T and zbar (the zonal ionic charge averaged over species, a surrogate for f). In this run, only the four outermost zones had their values perturbed from “nominal”.

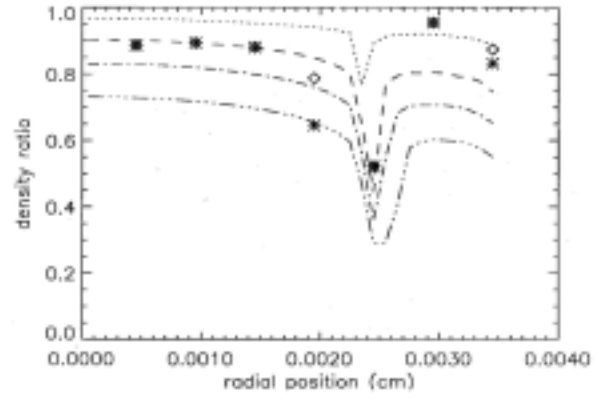


Fig. 2 Ratio of density at various TDG Dump times to density at first dump

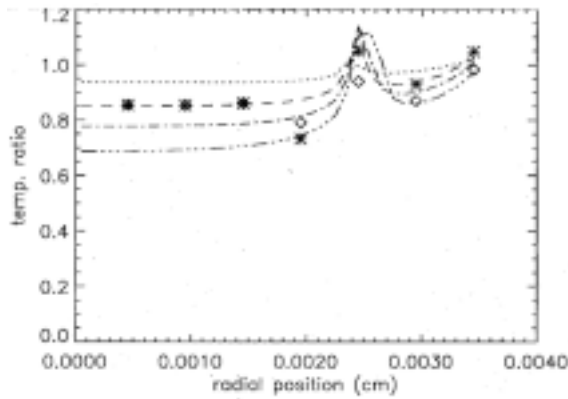


Fig. 3 Ratio of temperature at various TDG Dump times to temperature at first dump

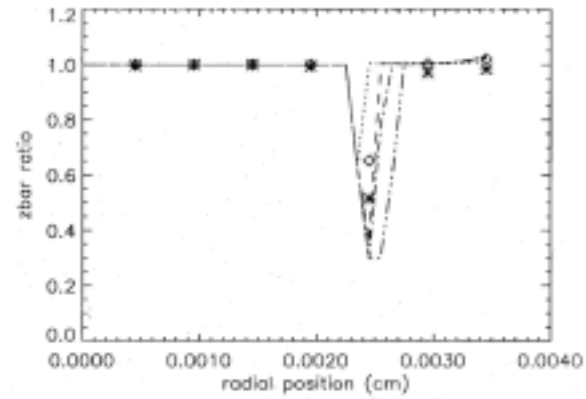


Fig. 4 Ratio of zbar at various TDG Dump times to zbar at first dump

### 3) Conclusions

Attenuation by cold, non-emitting dense matter is important for quantitative agreement. The fluence has very little contribution from the fuel—virtually all emission comes from carbon ( $Z^4$  dependence of BF emission). This is both good (mix easily diagnosed) and bad (unmixed fuel almost invisible). The highly non-linear dependence of fluence on T ( $\sim T^4$ ), and  $\rho$  ( $\sim \rho^2$ ) is both good (high sensitivity), and bad (real life nonspherical emission).

The high density and discontinuity at the interface creates a hump in lineouts for the no-mix case, not generally seen in real life—implying substantial mix. This hump is hard to deal with numerically. One must go low (in T,  $\rho$ , fluence) outside to get acceptable fluence inside. If the values of measured fluence had no uncertainty, then the answers for  $\rho$ , T, and f would be unique. But the  $\pm 15\%$  band of uncertainty around measured fluences allows for a corresponding non-uniqueness in answers. This issue manifests itself most easily with values for T and  $\rho$  that deviate in opposite directions from optimal. This is because increasing one while decreasing the other tends to leave fluence unchanged. Reducing the fluence uncertainties is the only solution. The Newton algorithm is typically most robust when underestimates are used as starting values. For deviations larger than 10% in T, or 20% in  $\rho$ , the Newton procedure will need supplemental preconditioning, for instance, by minimization or bisection algorithms.

Although the run described above did not have explicit mix, a run which did have substantial mix was analyzed. This revealed that the use of frequencies spanning just 1keV

(i.e. 3keV to 4keV) was too narrow. This is because the spectrum is too linear over this small a range, thus a third frequency does not add information. Equivalently, the determinant of the linearized 3 equations for a given LOS is close to zero, and the solution is not unique. What is needed is a curvature to the spectrum. Then the third frequency gives nontrivial information. Preliminary results indicate that 3 frequencies spread over 2keV (e.g., 3keV to 5keV) should suffice.

The key theoretical input to this algorithm is the opacity (and its derivatives with respect to  $T$ ,  $\rho$ , and  $f$ ). Although the results above utilized LTE continuum radiation as the observable, there is still some uncertainty in this opacity (associated with k-shell carbon). I have done an uncertainty analysis among 3 different opacity algorithms (average atom, tabular opacities with highly accurate BF, and in-line multi-sequence hydrogenic Saha calculations). The uncertainty analysis involved purposefully mismatching the opacities used by the post-processor code with those used by Newton. The results indicate that no major problems occur for tables (TDG) versus in-line hydrogenic Saha (Newton) ( $<3\%\Delta T$ ,  $<8\%\Delta\rho$ ), but that serious problems result when an average atom is used in TDG, but either detailed tables or in-line hydrogenic is used in Newton.

Work performed under the auspices of the U.S.DOE. by LANL under Contract W-7504-ENG-36.

## References

- [1] Greg Pollak, *et al*, Bull. Of APS (DPP)(1999), JO2 15.
- [2] Y. Ochi, *et al*, JQSRT, **65**, 393 (2000).
- [3] Greg Pollak, *et al*, JQSRT, **51**, 303, (1994).
- [4] E. Forster, K.Gabel, and I. Uschmann, Laser and Particle Beams, **9**, 135 (1991).
- [5] E. Forster, *et al*, JQSRT, **51**, 101, (1994).
- [6] I. Uschmann, *et al*, Rev. Sci. Instrum., **66**, 734 (1995).
- [7] M. Vollbrecht, *et al*, JQSRT, **58**, 965 (1997).
- [8] K. Fujita, *et al*, JQSRT, **58**, 585 (1997).
- [9] William Press, *et al*, *Numerical Recipes*, Cambridge (1989) p. 269.